ACS Catalysis

Letter

pubs.acs.org/acscatalysis

Understanding the Optimal Adsorption Energies for Catalyst Screening in Heterogeneous Catalysis

Bo Yang,[†] Robbie Burch,[†] Christopher Hardacre,*[,†] Gareth Headdock,[‡] and P. Hu*[,†]

[†]CenTACat, School of Chemistry & Chemical Engineering, The Queen's University of Belfast, Belfast, BT9 5AG, United Kingdom

[‡]Johnson Matthey Catalysts, PO Box 1, Billingham, Teesside, TS23 1LB, United Kingdom

Supporting Information

ABSTRACT: The fundamental understanding of the activity in heterogeneous catalysis has long been the major subject in chemistry. This paper shows the development of a two-step model to understand this activity. Using the theory of chemical potential kinetics with Brønsted–Evans–Polanyi relations, the general adsorption energy window is determined from volcano curves, using which the best catalysts can be searched. Significant insights into the reasons for catalytic activity are obtained.

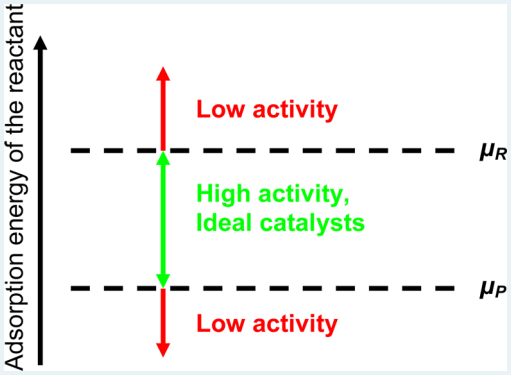

KEYWORDS: *heterogeneous catalysis, Brønsted–Evans–Polanyi relation, volcano curve, two-step model, adsorption energy window, catalyst design, chemical potential*

1. INTRODUCTION

Heterogeneous catalysis is of critical importance in energy conversion technologies, such as oil refining, fuel cells, and solar cells, as well as in the fine chemicals and pharmaceutical industries. A significant goal in this area is the use of theory not only to understand the adsorption, complex reaction and desorption processes, and thus provide explanations for experimentally observed phenomena, but also to design new catalysts for experimental testing. Among the current methods employed to perform this type of catalyst prediction, the evaluation of the Brønsted–Evans–Polanyi (BEP) relation and the volcano curve are the most frequently used.

Regarding the BEP relation, it was proposed that there should be a linear correlation between the reaction barrier and the enthalpy change of the elementary reaction steps.[1,2] Previous research, including ours, has reported some general linear relations between activation energies and enthalpy changes for dissociative and associative reactions calculated from density functional theory (DFT), in line with the classical BEP relations. Furthermore, an extended BEP relation was established between the transition state energy and the initial (final) state energy for the associative (dissociative) reactions, with the energies referenced to the gas phase reactant(s).[3−15] Therefore, the BEP relation provides the possibility of estimating the reaction barriers (transition state energies) from the corresponding enthalpy changes (initial/final state energies).This is important because the calculation of the enthalpy changes (initial/final state energies) of the elementary steps is much more efficient than determining the reaction barriers.

The volcano curve provides a relationship between the catalytic activities and the adsorption energies of a given reactant on the catalyst surface. The volcano curve is typically explained by the Sabatier principle, which states that the adsorption of the reactants on the catalyst surface should be neither too strong nor too weak to achieve high activity.[16] This has also been exemplified using experimentally determined catalytic activity plotted as a function of the adsorption energy of specific species calculated from DFT in which volcano type curves were obtained.[17−19] A recent study from our group proposed to understand volcano curves from the perspective of surface free sites, and a new insight was obtained.[20] Moreover, volcano type curve can be obtained by utilizing the BEP linear relations without barrier calculations. Furthermore, it was demonstrated that multiphase catalysts can be understood using a three-dimensional volcano plot.[21]

Typically, new catalysts are developed by trial-and-error approaches experimentally, whereas DFT calculations have been shown to be possible for catalyst design/screening by computing adsorption energies or reaction barriers for catalytic processes.[22] However, the theoretical catalyst design/screening processes may be further accelerated with more detailed analyses on the BEP relation and the volcano curve as well as

Received: August 24, 2013
Revised: December 2, 2013
Published: December 9, 2013

the models developed over the past decade. For example, a kinetics theory based on chemical potential was developed in our group recently for heterogeneous catalysis and shows significant potential for catalyst design for dye-sensitized solar cells.[23−25] In this approach, the total energy profile was converted to the profile of chemical potential, and an explanation of the universality of the adsorption energy window in heterogeneous catalysis was proposed.[6,8] In the current work, we analyze in detail the volcano curves derived from the two-step model,[9,23,26] aiming to obtain a new understanding of the chemical potential kinetics as well as the adsorption energy window for optimal catalysts. It should be noted that an approach similar to the two-step model used in the current work was recently employed by Koper[27] to understand electrocatalytic reaction processes. In this case, the potential-determining step should be considered for an electrocatalytic process.

2. RESULTS AND DISCUSSION

Taking the two-step model reported in our recent work as a starting point to describe heterogeneously catalyzed reactions, namely, the adsorption of reactants to form the intermediates and the desorption of the intermediate to the products[9,23,26]

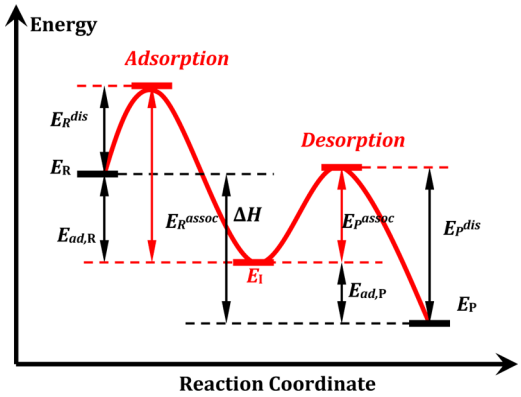

Figure 1. Schematic profile of the two-step model taking into consideration the dissociative adsorption of reactants and associative desorption of products on a heterogeneous catalyst surface. ΔH is the enthalpy change of the overall reaction. E_R and E_P are total energies of the gaseous reactants and products, respectively. $E_{ad,R}$ and $E_{ad,P}$ are the adsorption energies of the reactants and the products, respectively. E_R^{dis} and E_R^{assoc} are the barriers for the adsorption and the corresponding reverse reaction of the reactants, respectively. Similarly, E_P^{dis} and E_P^{assoc} are the barrier of desorption and the corresponding reverse reaction of the products, respectively. E_I is the energy of the intermediate state.

(the energy profile of the two steps is shown in Figure 1), the following equations can be obtained:

$$\begin{aligned}\Delta H &= E_P - E_R \\ &= (E_I - E_R) - (E_I - E_P) \\ &= E_{ad,R} - E_{ad,P}\end{aligned} \quad (1)$$

$$E_R^{assoc} = E_R^{dis} - E_{ad,R} \quad (2)$$

$$E_P^{assoc} = E_P^{dis} - E_{ad,P} \quad (3)$$

where ΔH is the enthalpy change of the overall reaction. $E_{ad,R}$ and $E_{ad,P}$ are the adsorption energies of the reactants and the products, respectively. E_R^{dis} and E_R^{assoc} are the barriers for the adsorption and the corresponding reverse reaction, respectively. Similarly, E_P^{dis} and E_P^{assoc} are the barriers for desorption and the reverse reaction, respectively.

Using the BEP relation, we can write

$$E_R^{dis} = a_R E_{ad,R} + b_R \quad (4)$$

$$E_P^{dis} = a_P E_{ad,P} + b_P \quad (5)$$

where a_R, a_P, b_R, and b_P are constants. One can obtain the reaction rate of the overall reaction as[9,28]

$$r = \frac{k_B T}{h} \frac{1}{\frac{P^0}{P_R} e^{S_R/R} e^{E_R^{dis}/RT} + \frac{P_P}{P_R} e^{\Delta G/RT} e^{E_R^{assoc}/RT}}$$

if adsorption is the rate-determining step (6)

$$r = \frac{k_B T}{h} \frac{1}{\frac{P^0}{P_R} e^{S_R/R} e^{E_{ad,R}+E_P^{assoc}/RT} + e^{E_P^{assoc}/RT}}$$

if desorption is the rate-determining step (7)

where k_B and h are constants, and T is the reaction temperature. P^0, P_R, and P_P are the standard pressure, partial pressure of the reactants, and partial pressure of the products, respectively. ΔG is the free energy change of the overall reaction. S_R is the entropy of the reactants. The details for the derivation of eqs 6 and 7 can be obtained from ref 9 and the Supporting Information (SI).

Because E_R^{dis}, E_R^{assoc}, E_P^{dis}, and E_P^{assoc} are all related to the adsorption energies of the reactants ($E_{ad,R}$) or the products ($E_{ad,P}$) via the BEP relations (eqs 2−5) and both adsorption energies are further related to the enthalpy change of the reaction (eq 1), we can establish that the reaction rates will only be determined by the $E_{ad,R}$ for a given set of reaction conditions. Therefore, correlating the reaction rates with the adsorption energies of the reactants ($E_{ad,R}$) gives rise to the volcano curves shown in Figure 2. We can see the following striking features: (i) There are three volcano curves, namely the curves obtained from the adsorption being the rate-determining step (red), the desorption being the rate-determining (blue), and the overall one achieved from combining both the adsorption and desorption processes (black), respectively. (ii) In regions 1 and 2, the rates from the adsorption being rate-determining are overestimated (they are above the overall rates), whereas the rates from the adsorption are almost the same as the overall one (they overlap each other after $E_{ad,R,max3}$) in regions 3 and 4. The opposite is true for the desorption one. (iii) There is only one maximum in the reaction rates associated with the adsorption being the rate-determining step, and this is also true if the desorption is the rate-determining step. Correspondingly, $E_{ad,R,max1}$, $E_{ad,R,max2}$, and $E_{ad,R,max3}$ are the adsorption energies of the reactants when the adsorption rate reaches the maximum, the desorption rate reaches the maximum, or where the overall rate reaches the maximum, respectively.

Interestingly, the values of $E_{ad,R,max1}$ and $E_{ad,R,max2}$ can be determined analytically by solving the following partial differentiatials:

dx.doi.org/10.1021/cs400727f | ACS Catal. 2014, 4, 182−186

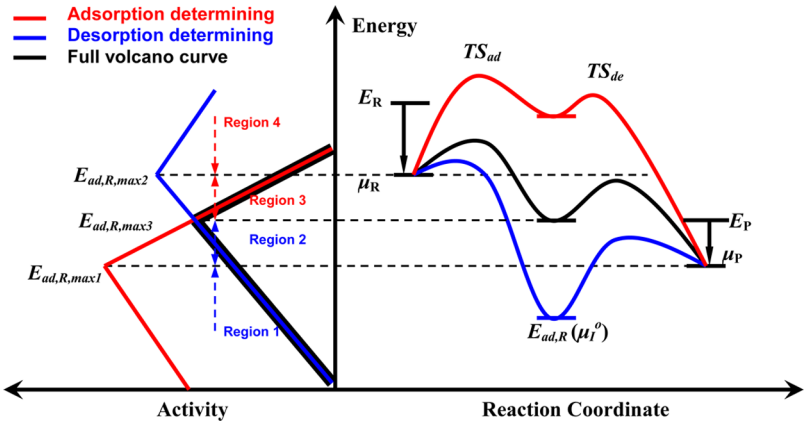

Figure 2. Schematic diagram of the volcano curves associated with reactions in which the adsorption (red) and desorption (blue) are rate-determining, together with the real volcano curve (black) (left). The right side of the figure shows the energy profiles on three typical catalysts. μ_R and μ_P are the chemical potentials of the gaseous reactants and products, respectively.

$$\frac{\partial\left[\frac{P^0}{P_R}e^{S_R/R}e^{E_R^{dis}/RT}+\frac{P_P}{P_R}e^{\Delta G/RT}e^{E_R^{assoc}/RT}\right]}{\partial(E_{ad,R})_{T,P_R,P_P}}=0 \tag{8}$$

$$\frac{\partial\left[\frac{P^0}{P_R}e^{S_R/R}e^{E_{ad,R}+E_P^{assoc}/RT}+e^{E_P^{assoc}/RT}\right]}{\partial(E_{ad,R})_{T,P_R,P_P}}=0 \tag{9}$$

Combining eqs 1−5, 8, and 9, eqs 10 and 11 are obtained.

$$E_{ad,R,max\,1}=RT\ln\left(\frac{1-a_R}{a_R}\right)+RT\ln\left(\frac{P_P}{P^0}\right)-TS_R+\Delta G \tag{10}$$

$$E_{ad,R,max\,2}=RT\ln\left(\frac{1-a_P}{a_P}\right)+RT\ln\left(\frac{P_R}{P^0}\right)-TS_R \tag{11}$$

In addition, $E_{ad,R,max3}$ is the cross-point between the adsorption-determining and desorption-determining curves and, thus, can also be obtained by combining eqs 6 and 7.

$$E_{ad,R,max\,3}=\frac{RT\ln\left(\frac{P_R}{P^0}\right)+b_P-b_R-TS_R+(1-a_P)\Delta H}{1+a_R-a_P} \tag{12}$$

Compared with $E_{ad,R,max1}$ and $E_{ad,R,max2}$, which consist of a_R and a_P, respectively, $E_{ad,R,max3}$ contains more variables, such as b_R and b_P. Because a_R and a_P are well-known to be around 0−1 for most reactions but b_R and b_P need to be determined from a set of catalysts, $E_{ad,R,max1}$ and $E_{ad,R,max2}$ may be more easily used.

After careful examination of the curves in Figure 2, we can achieve the following trends:

(i) When the reactants interact with the catalyst surface very strongly, shown as region 1 in Figure 2 (i.e., where $E_{ad,R} < E_{ad,R,max1}$), it will result in energy profiles in the lower area on the right-hand side of Figure 2, such as the blue energy profile, and the free site coverage should be low at the steady state, leading to a low reaction rate due to reactant poisoning.

(ii) When the interaction between the reactants and the catalyst surface is too weak, indicated as region 4 (i.e., where $E_{ad,R} > E_{ad,R,max2}$), the reaction is governed by energy profiles in the upper area on the right-hand side of Figure 2, such as the red energy profile, and low steady state coverage of reactants on the surface will be formed, also leading to a low rate of reaction.

(iii) When the adsorption energy of the reactants shifts to regions 2 and 3 in Figure 2 (i.e., where $E_{ad,R,max1} < E_{ad,R} < E_{ad,R,max2}$), the surface has the ideal coverage of the adsorbed species and free sites so that both the adsorption of reactants on the surface and the desorption of products from the surface are facile.

Having obtained the two critical adsorption energies, $E_{ad,R,max1}$ and $E_{ad,R,max2}$, we are in a position to quantitatively address the adsorption energy window: Nørskov and co-workers discovered that there is a universal adsorption energy window within which the excellent catalysts can be found for several reactions.[6,8] Since this is such an important result, it is worth discussing whether our framework in the current work can provide any insight into this issue. From the above detailed analyses, we can suggest that the optimal catalysts for a given reaction condition should have reactant adsorption energies within the energy range between $E_{ad,R,max1}$ and $E_{ad,R,max2}$, as denoted by eqs 10 and 11. By applying the chemical potentials of gaseous species (see equation S3 in the SI) to eqs 10 and 11, we can readily obtain

$$E_{ad,R,max\,1}=RT\ln\left(\frac{1-a_R}{a_R}\right)+\mu_P-H_R \tag{13}$$

$$E_{ad,R,max\,2}=RT\ln\left(\frac{1-a_P}{a_P}\right)+\mu_R-H_R \tag{14}$$

where μ_R and μ_P are the chemical potentials of the reactants and products, respectively. Because the energy of the gaseous reactants is usually taken to be zero as a reference point in potential energy profiles, H_R can be eliminated from eqs 13 and 14. Using the fact that $E_{ad,R,max1} < E_{ad,R} < E_{ad,R,max2}$, as discussed above, we can write the following equation for optimal catalysts:

$$\mu_R+RT\ln\left(\frac{1-a_P}{a_P}\right)>E_{ad,R}>\mu_P+RT\ln\left(\frac{1-a_R}{a_R}\right) \tag{15}$$

It is clear from eq 15 that the optimal adsorption energy of the reactant is determined by μ_R, μ_P, a_R, and a_P. It is known that

dx.doi.org/10.1021/cs400727f | ACS Catal. 2014, 4, 182−186

a_R is close to 1, with a typical range of 0.8−1,[4,6,7,9,23] and our previous work showed that a_P is around 0.3.[9] Taking a_R and a_P as 0.9 and 0.3, respectively, as an example, the terms $RT \ln(1 - a_R/a_R)$ and $RT \ln(1 - a_P/a_P)$ are −0.09 and 0.04 eV at 500 K, respectively, and it follows that

$$\mu_R + 0.04 > E_{ad,R} > \mu_P - 0.09 \quad (16)$$

This means that the optimal adsorption energy window is from μ_R + 0.04 to μ_P − 0.09. Interestingly, using the theory of chemical potential kinetics and the surface free sites, a recent study from our group[23] derived an adsorption energy window to be $\mu_R + \varepsilon > E_{ad,R} > \mu_P - \varepsilon$, where ε is about 0.1−0.2 eV for 500 K, which is very close to the current work. It is worth noting that the energy window in the current work is analytically derived from the maxima of volcano curves obtained from the two-step model coupled with the BEP relation without any other assumptions. If one goes one step further, a simple adsorption window of $\mu_R > E_{ad,R} > \mu_P$ can be obtained, omitting the small energies of 0.04 and −0.09 eV.

It is clear from the discussion above that $E_{ad,R,max1}$ and $E_{ad,R,max2}$ from eqs 10 and 11 are of great importance to the activity of catalysts for a given reaction. Hence, it is worth discussing the physical meanings of these two terms. We can see from eqs 10 and 11 that the parameters expressing $E_{ad,R,max1}$ and $E_{ad,R,max2}$ fall into three groups: (i) the reaction conditions, such as P_R, P_P, and temperature; (ii) the thermodynamic parameters, including ΔG and S_R; and (iii) the kinetic parameters, for example, a_R and a_P. However, the contribution from kinetic parameters to $E_{ad,R,max1}$ and $E_{ad,R,max2}$ is very small, $RT \ln(1 - a_R/a_R)$ and $RT \ln(1 - a_P/a_P)$, which are only −0.09 and 0.04 eV, respectively, as discussed above. The kinetic contribution to $E_{ad,R,max1}$ and $E_{ad,R,max2}$ is so small that it can be omitted, and thus, they will be determined by only the reaction conditions and the thermodynamic parameters. This is a very surprising result, considering that $E_{ad,R,max1}$ and $E_{ad,R,max2}$ are derived from reaction kinetics.

It should be noted that there are some limitations in the model described. First, our model can be applied only to the systems having the same mechanism for each of the catalysts screened. Second, it is assumed that there is only one rate-determining step in the system, whereas in real systems, there may be more than one rate-limiting step. Therefore, our model is a simplified description of real systems, and it may be valid for only some real systems. Despite the limitations, it does provide an approach to rapidly screen catalysts for a given reaction. Future comparisons with experimental data will provide some guidance as to the accuracy of the predictions from the model.

3. CONCLUSIONS

In summary, a two-step model has been used to gain insight into the kinetics of heterogeneous catalytic reactions. Optimal adsorption energies of reactants for (i) the overall reaction ($E_{ad,R,max3}$); (ii) assuming that the adsorption is the rate-determining step ($E_{ad,R,max1}$); and (iii) assuming that the desorption process is the rate-determining step ($E_{ad,R,max2}$) are analytically obtained. The best catalysts appear to be located between $E_{ad,R,max1}$ and $E_{ad,R,max2}$, and the energy window to search for optimal catalysts is derived as $\mu_R + 0.04 > E_{ad,R} > \mu_P - 0.09$ or simply $\mu_R > E_{ad,R} > \mu_P$. Insights into the activity of heterogeneous catalytic reactions are obtained.

■ ASSOCIATED CONTENT

Supporting Information

Derivation of the reaction rates of the adsorption and desorption determining processes and the derivation of the relation between the adsorption energy window and the chemical potential window. This material is available free of charge via the Internet at http://pubs.acs.org.

■ AUTHOR INFORMATION

Corresponding Authors

*E-mail: c.hardacre@qub.ac.uk.
*E-mail: p.hu@qub.ac.uk.

Notes

The authors declare no competing financial interest.

■ ACKNOWLEDGMENTS

This work is financially supported by EPSRC and Johnson Matthey through the CASTech program (EP/G012156/1). We acknowledge helpful discussions with Dr. Jun Cheng (University of Cambridge/University of Aberdeen), and B.Y. is thankful for the financial support of a Dorothy Hodgkin Postgraduate Award (DHPA) studentship jointly funded by EPSRC and Johnson Matthey.

■ REFERENCES

(1) Brønsted, J. N. *Chem. Rev.* **1928**, *5*, 231.
(2) Evans, M. G.; Polanyi, M. *Trans. Faraday Soc.* **1938**, *34*, 11.
(3) Pallassana, V.; Neurock, M. *J. Catal.* **2000**, *191*, 301.
(4) Logadottir, A.; Rod, T. H.; Nørskov, J. K.; Hammer, B.; Dahl, S.; Jacobsen, C. J. H. *J. Catal.* **2001**, *197*, 229.
(5) Liu, Z. P.; Hu, P. *J. Chem. Phys.* **2001**, *115*, 4977.
(6) Nørskov, J. K.; Bligaard, T.; Logadottir, A.; Bahn, S.; Hansen, L. B.; Bollinger, M.; Bengaard, H.; Hammer, B.; Sljivancanin, Z.; Mavrikakis, M.; Xu, Y.; Dahl, S.; Jacobsen, C. J. H. *J. Catal.* **2002**, *209*, 275.
(7) Michaelides, A.; Liu, Z. P.; Zhang, C. J.; Alavi, A.; King, D. A.; Hu, P. *J. Am. Chem. Soc.* **2003**, *125*, 3704.
(8) Bligaard, T.; Nørskov, J. K.; Dahl, S.; Matthiesen, J.; Christensen, C. H.; Sehested, J. *J. Catal.* **2004**, *224*, 206.
(9) Cheng, J.; Hu, P.; Ellis, P.; French, S.; Kelly, G.; Lok, C. M. *J. Phys. Chem. C* **2008**, *112*, 1308.
(10) Nørskov, J. K.; Bligaard, T.; Hvolbæk, B.; Abild-Pedersen, F.; Chorkendorff, I.; Christensen, C. H. *Chem. Soc. Rev.* **2008**, *37*, 2163.
(11) Loffreda, D.; Delbecq, F.; Vigné, F.; Sautet, P. *Angew. Chem., Int. Ed.* **2009**, *48*, 8978.
(12) van Santen, R. A.; Neurock, M.; Shetty, S. G. *Chem. Rev.* **2010**, *110*, 2005.
(13) Gong, X. Q.; Liu, Z. P.; Raval, R.; Hu, P. *J. Am. Chem. Soc.* **2004**, *126*, 8.
(14) Yang, B.; Burch, R.; Hardacre, C.; Headdock, G.; Hu, P. *ACS Catal.* **2012**, *2*, 1027.
(15) Yang, B.; Gong, X.-Q.; Wang, H.-F.; Cao, X.-M.; Rooney, J. J.; Hu, P. *J. Am. Chem. Soc.* **2013**, *135*, 15244.
(16) Sabatier, P. *Ber. Dtsch. Chem. Ges.* **1911**, *44*, 1984.
(17) Toulhoat, H.; Raybaud, P. *J. Catal.* **2003**, *216*, 63.
(18) Guernalec, N.; Geantet, C.; Cseri, T.; Vrinat, M.; Toulhoat, H.; Raybaud, P. *Dalton Trans.* **2010**, *39*, 8420.
(19) Over, H.; Schomäcker, R. *ACS Catal.* **2013**, *3*, 1034.
(20) Wang, H.; Guo, Y.; Lu, G.; Hu, P. *J. Chem. Phys.* **2009**, *130*, 224701.
(21) Cheng, J.; Hu, P. *J. Am. Chem. Soc* . **2008**, *130*, 10868.
(22) Studt, F.; Abild-Pedersen, F.; Bligaard, T.; Sørensen, R. Z.; Christensen, C. H.; Nørskov, J. K. *Science* **2008**, *320*, 1320.
(23) Cheng, J.; Hu, P. *Angew. Chem., Int. Ed.* **2011**, *50*, 7650.

(24) Hou, Y.; Wang, D.; Yang, X. H.; Fang, W. Q.; Zhang, B.; Wang, H. F.; Lu, G. Z.; Hu, P.; Zhao, H. J.; Yang, H. G. *Nat. Commun.* **2013**, *4*, 8.
(25) Zhang, B.; Wang, D.; Hou, Y.; Yang, S.; Yang, X. H.; Zhong, J. H.; Liu, J.; Wang, H. F.; Hu, P.; Zhao, H. J.; Yang, H. G. *Sci. Rep.* **2013**, *3*, 7.
(26) Yang, B.; Burch, R.; Hardacre, C.; Headdock, G.; Hu, P. *J. Catal.* **2013**, *305*, 264.
(27) Koper, M. T. M. *J. Solid State Electrochem.* **2013**, *17*, 339.
(28) Dumesic, J. A. *J. Catal.* **1999**, *185*, 496.

dx.doi.org/10.1021/cs400727f | *ACS Catal.* 2014, 4, 182−186